Optimizing a Three-stage Autofocus System for Synthetic Aperture Imaging using a UUV

T. J. Sutton, H. D. Griffiths
University College London
Torrington Place
London WC1E 7JE
UK
t.sutton@meng.ucl.ac.uk
h.griffiths@ee.ucl.ac.uk

S. A. Chapman
QinetiQ Bincleaves
Newtons Road
Weymouth DT4 8UR
UK
sachapman@qinetiq.com

R. Crook, M. Way
Thales Underwater Systems
Ocean House
Templecombe BA8 0DH
UK
Rob.Crook@uk.thalesgroup.com

***Abstract*-High-resolution synthetic aperture imaging of the seabed at ranges up to 500 m requires precise compensation for vehicle motion errors. The paper shows how a combination of (a) direct measurement, (b) DPCA autofocus (*i.e.* cross-correlation of overlapping phase centres) and (c) Phase Gradient Autofocus provide a robust, three-stage motion compensation scheme. The performance and reliability of the three-stage scheme depend on the degree of overlap between pings, the length of the synthetic aperture and a number of key parameters that are chosen for the DPCA and PGA algorithms. Results are presented in the context of a set of UUV trials in shallow coastal waters using a vehicle of 7m length equipped with a 1.1 m array of 192 hydrophones. Despite a water depth of only 12 m with consequent severe problems due to multipath reflections, images were obtained of target objects at ranges in excess of 250 m with resolutions of a few tens of millimeters.**

I. INTRODUCTION

The concept of synthetic aperture sonar is not new, but the widespread development of AUVs for long-range SAS imaging has been held up by the need for reliable motion compensation methods. In a high-resolution imaging system operating at over 100 kHz, errors of as little as a few millimeters in the nominal location of the hydrophone array can cause appreciable defocus. Direct position measurement using an onboard inertial navigation system (INS) is generally not adequate [1]. It is necessary to use the measured sonar data itself to focus the image ('autofocus'). Both the DPCA (displaced phase centers antenna) algorithm and the PGA (phase gradient autofocus) algorithm have been considered for this purpose. In this paper we discuss the use of direct measurement, DPCA and PGA in combination to focus the results of a set of UUV trials. This combined approach to autofocus has also been discussed by Chang *et al* [2].

Earlier studies using rail-based systems [3] laid the groundwork for a series of trials led by QinetiQ that took place in 2001 using a large unmanned underwater vehicle, 7 m in length. An array of 192 hydrophones was used to sample the sound field due to a set of targets placed at a range of several hundred meters in shallow water close to the shore. UCL have analysed the data from these trials as part of an EPSRC/TUS/QinetiQ project to investigate motion compensation techniques for synthetic aperture sonar. Using a three-stage approach to autofocus, targets at a range of 262m have been imaged with a resolution of less than 100 mm.

II. UUV TRIALS, 2001

Under the former DERA Priority Pathfinder scheme for jointly funded research, a three-year project was set up to investigate how to integrate a high-quality wideband minehunting sonar into a 21" diameter UUV. The project partners were QinetiQ, Thales Underwater Systems and BAE Systems. The vehicle was some 7m in length and propelled at 1-2 m/s using internal batteries (Figure 1). Communication and data transfer to the surface was through a high-bandwidth (2.5 Gbit/s) optical fiber link, as the vehicle was designed before the recent rapid development in the capacity of hard disc drives.

Fig. 1. The UUV mine reconnaissance demonstrator

Figure 2 shows the installed side-looking transmitter and hydrophone array. The transmitter was designed to be capable of illuminating a 90 deg horizontal arc. The receiver comprised six 32-element linear hydrophone arrays placed in a line to give an array of 192 hydrophones. The separation of the hydrophones was 5.8 mm, giving a total array length of 1.1 m. At the carrier frequency, the physical beamwidth available with the array was about 0.5 degree. The sonar data were demodulated digitally and then downsampled to 75 kHz for subsequent analysis.

Fig. 2. Configuration of side-looking sonar transmitter (curved) and hydrophone array

For the trials discussed here, the vehicle was run at 1 m/s transmitting chirp pulses with repetition intervals of 0.5 s ('run3a') or 0.25 s ('run 7') giving a maximum unambiguous range of 368 m or 184 m respectively. The spatial sampling factor α is given by:

$$\alpha = \frac{L}{2VT_{pri}} \tag{2.1}$$

(L: length of hydrophone array; V: vehicle speed; T_{pri}: pulse repetition interval.) For the trials α was 1.2 for run 3a, or 2.3 for run 7, indicating a rather low overlap of redundant phase centers for DPCA autofocus. (The optimum value for sway and yaw estimation is α = 4 [4]; α = 1 corresponds to no overlap at all.)

III. MOTION COMPENSATION AND IMAGING

Figure 3 shows the calculation scheme for motion compensation and imaging. There are three stages:

(1) Direct compensation. The motions measured by the INS are projected into the slant range plane and used to apply a time advance or delay to the measured sonar returns received at each hydrophone.

(2) DPCA. Phase centers that are nominally coincident from one ping to the next are cross-correlated to determine platform surge and sway, and again the results are applied as an advance or delay to the sonar returns at each hydrophone.

(3) PGA. Phase errors across the final image are extracted iteratively to obtain a focused final image.

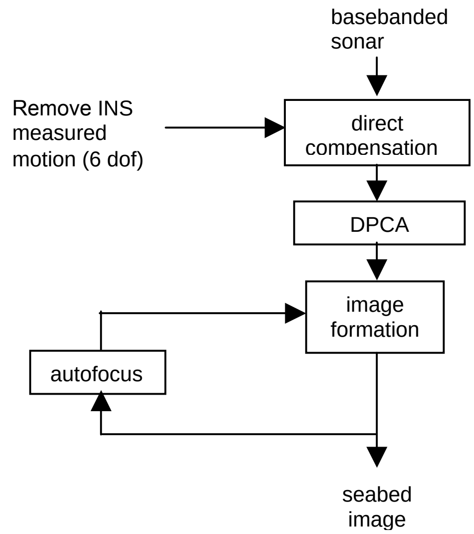

Fig. 3. Analysis scheme for synthetic aperture sonar

Each of these stages will now be discussed in more detail in the context of the UUV trials.

Direct compensation. The vehicle incorporated a Doppler Velocity Log and separate INS system positioned nearer the nose of the vehicle. Figure 4 shows the typical variations in yaw, pitch and roll of the UUV during a 76 second period of operation in a straight line. The vehicle was under continuous active closed-loop control during the period shown (and throughout the trials).

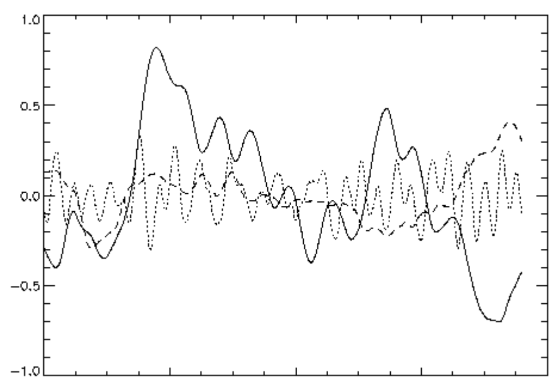

Fig. 4. Variations in yaw, pitch and roll of the UUV during a 76 sec period of operation in a straight line

The sway of each hydrophone is the sum of the sway measured directly by the INS and a lever-arm component due to the fact that the INS rotation is measured some 1.5 m away from the center of the hydrophone array.

DPCA. The concept of DPCA is well-established [5,6]. If the vehicle is not traveling too fast, phase centers from successive pings overlap, giving two measurements of the same scene from nominally the same point in space but at different times. Cross-correlation of the two time series shows whether the vehicle shifted its position across-track (toward or away from the scene) in the interval. If the overlap is sufficient it is possible to estimate the yaw as well [4]. In addition, the correlation coefficient falls away rapidly if the phase centers are displaced along the track [7]. In our trials the correlation fell from 80% to 40% when the phase centers were displaced along track by just 8 mm. Thus crosscorrelating each phase center from one ping with several nearby phase centers from the next ping gives an accurate means of measuring vehicle velocity along the track.

The correlation coefficient also fell as the range was increased: the coefficient was 80% at 40 m range, falling to 40% at 200 m range. In shallow water (just 12 m in the present case) the multipath reflections from the surface have an increasingly decorrelating effect as the range swath becomes more distant.

PGA. The phase gradient autofocus (PGA) algorithm was published by P.H. Eichel of Sandia National Labs New Mexico in 1989. (See [8] for a full description.) PGA is a method of extracting the phase error from a spotlight mode synthetic aperture radar image, that is, one in which the antenna is steered to maintain a chosen target area in view. Correction of the phase error focuses the image. In SAS, the phase error may be due to uncompensated across-track motion of the hydrophone array, medium inhomogeneity or any other source. If the hydrophone consists of a large number of small (essentially omnidirectional) hydrophones, the requirement to maintain the target area in view along the whole synthetic aperture is not restrictive.

Some care is required when implementing the PGA algorithm for SAS, because the range increments used for SAS are much narrower than those for SAR. As a result the response of a point scatterer after range compression will generally migrate through many range bins over the track length of interest. The application of PGA to SAS is discussed in [3].

Imaging Algorithm. There are several imaging algorithms that can be conveniently used to create a synthetic aperture image, including direct delay-and-sum, the wavenumber algorithm, fast factorised backprojection [9] and others. For the images shown here we used the range-Doppler algorithm with secondary range compression. (A valuable review of imaging algorithms for synthetic aperture sonar is given by Hawkins [10].) Typical track lengths were 15-20 m. The hydrophones were gathered into small groups (subapertures) to reduce the number of along-track samples.

III. TARGET IMAGES

Figure 5 shows a cylinder attached to a base at a range of 40 m. The track length (synthetic aperture) was 15 m. As seen from the inset photograph, the straps holding the cylinder in place show up clearly, along with its shadow across the seabed.

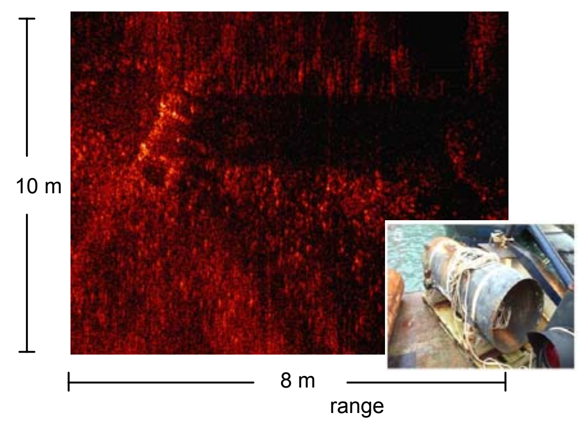

Fig. 5. Synthetic aperture image of a cylinder attached to a base at 40 m. (Run 7a)

Figure 6 shows a piece of unidentified debris on the seabed at about 40 m range.

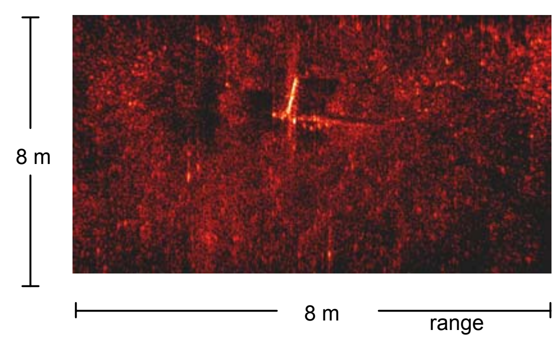

Fig. 6 Synthetic aperture image of debris on the seafloor at 40 m. (Run 7a)

Figure 7 shows a small, highly reflective sphere at a range of 207 m. Multiple images of the target are seen due to internal reflections in the sphere. The surrounding seabed is also seen to be in focus.

The point reflection is 38 dB above the surrounding seabed. The azimuth resolution is 90 mm.

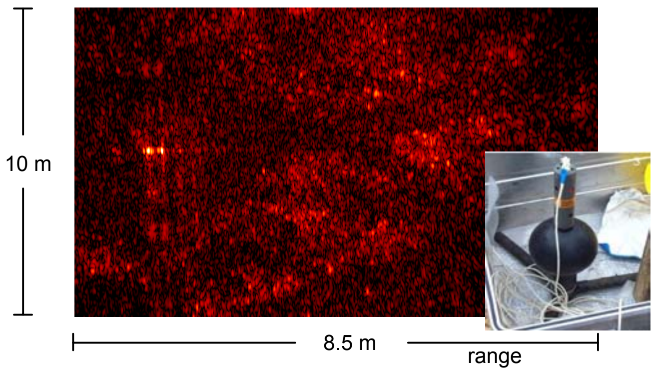

Fig. 7. Synthetic aperture image of a highly reflective sphere at 207 m. (Run 3a)

At long range the very shallow water conditions (12 m) the image starts to become hazy due to multipath reflection. Figure 8 shows a floating sphere supported by two concrete blocks at a range of 224 m. The blocks show up clearly, while the floating sphere does not form a clear image, apparently because it is moving in the water current. The haze one or two meters behind the target is thought to be due to multipath reflection from the (moving) sea surface, and obscures the expected shadow.

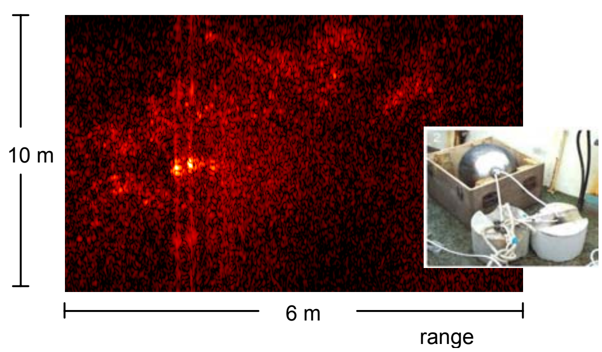

Fig. 8. Spotlight synthetic aperture image of a floating sphere at 224 m (Run 3a).

The furthest target that has been successfully imaged using these data is shown in Figure 9. It is a cylindrical mine-like object as shown in the photograph.

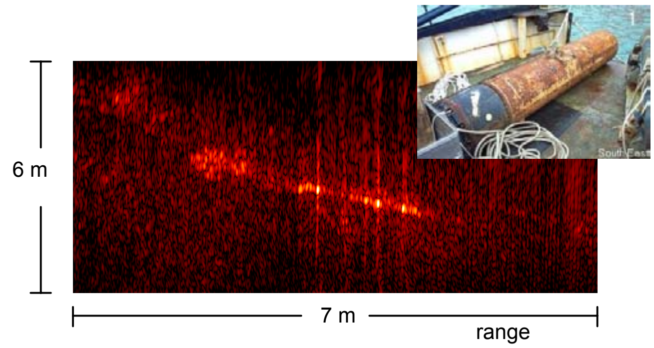

Fig. 9. Synthetic aperture image of a cylinder at 262 m. (Run 3a)

IV. OPTIMIZING THE MOTION COMPENSATION ALGORITHM

The AUV trials represented a considerable leap in conditions from the earlier rail-based trials discussed in [3]. Specifically, the vehicle speed was 1 m/s instead of 10 mm/s, an increase by a factor of 100. The range of targets successfully imaged extended to 260 m, compared with 75 m. In order to maintain a long unambiguous range the overlap factor α was reduced to 1.2. It was therefore not possible to use DPCA to estimate the yaw of the vehicle. On the other hand, the vehicle sway measured by DPCA was much more accurate (i.e. resulting in a much better SAS image) than the sway measured by the INS. In this case the INS was limited by (1) low frequency of measurement (one sample per second) and (2) uncertainty over the placement of the INS, introducing error into the lever-arm calculations.

At long range the correlation coefficients measured by DPCA fell substantially (Sect. III above), but the surge and sway estimations were still useful. It is worth noting that even if the accuracy of the DPCA motion estimation were unchanged, the defocus due to a given motion error would increase with range [11].

PGA is an iterative method in which a relatively strong scatterer is chosen for each range line and a window function is applied to exclude other contributions. The closer the image is to being in focus, the narrower the window and the more accurate the estimation of phase error. Thus PGA might not converge at all if the defocus is too large at the outset; on the other hand it converges rapidly if the image is close to being in focus. Therefore, in using PGA it is essential first to use an algorithm such as DPCA to remove most of the motion error.

It was found that, in cases where neither the INS nor DPCA were used to provide yaw compensation, the PGA algorithm determined an across-track displacement correction whose *slope* was similar to the measured yaw of the hydrophone array.

The PGA algorithm includes an assumption about the image, namely, that the focused image contains a large number of point-like scatterers. (Thus a single 'prominent point' is not required, but the image should have adequate texture or contrast.) This assumption turns out to be valid in practice and tends to offset the problems of using DPCA at long range.

VI CONCLUSION

Synthetic aperture images of target objects have been calculated to a distance in excess of 250 m using data obtained from a UUV traveling at 1 m/s over track lengths of 10-20 m. Use of a large number of small hydrophones ensured a wide field of view (+/- 40 degrees). A three-stage motion compensation algorithm has been demonstrated comprising direct measurement with an INS, displaced phase centers antenna and phase gradient autofocus applied in turn. Direct measurement of yaw using the INS was found to obviate the need for yaw estimation by DPCA, allowing the use of a low overlap factor. When the yaw compensation was omitted altogether the PGA algorithm determined an additional across-track displacement correction whose slope was similar to the measured yaw.

REFERENCES

[1] B.D. Huxtable and E.M. Geyer, 'Motion compensation feasibility for high resolution synthetic aperture sonar.' *Proc IEEE Oceans 93*, I 125-131.

[2] E. Chang, D.S. Marx, M.A. Nelson, W.D. Gillespie, A. Putney, L.K. Warman, R.E. Chatham and B.N Barrett, 'Long range active synthetic aperture sonar results' *Proc IEEE Oceans 2000*, I pp1-5

[3] T.J. Sutton, H.D. Griffiths, A.P. Hetet, Y. Perrot and S.A. Chapman, 'Experimenal validation of autofocus algorithms for high-resolution imaging of the seabed using synthetic aperture sonar.' *IEE Proceedings – Radar, Sonar, Navig*. Vol 150 (2), Apr 2003, pp78-83.

[4] A. Bellettini and M.A. Pinto, 'Theoretical accuracy of synthetic aperture sonar micronavigation using a displaced phase centers antenna.' IEEE Journal of Oceanic Engineering Vol 27 (4), Oct 2002, pp780-789.

[5] R.W. Sheriff, 'Synthetic aperture beamforming using automatic phase compensation of high frequency sonars.' Proc 1992 Symposium on autonomous underwater vehicle Technology, June 1992, 238-245.

[6] M.A. Pinto, F. Fohanno, O. Tremois and S. Guyonic 'autofocusing a synthetic aperture soanr using the temporal and spatial coherence of seabfloor reverberation.' in *High frequency acoustics in shallow water*, ed N. G. Pace (1997) (Saclantcen Conf. Proc. CP-45), 417-424.

[7] Y. Doisy, 'General Motion Estimation from Correlation Sonar.' *IEEE Journal of Oceanic Engineering*, Vol 23 (2), April 1998.

[8] C.V. Jakowatz, Jr, D.E. Wahl, P.H. Eichel, D.C. Ghiglia and P.A. Thompson, *Spotlight-mode synthetic aperture radar: A signal processing approach*, Kluwer Academic Publishers, 1996.

[9] S.M. Banks and H.D. Griffiths, 'The use of fast factorised back projection for synthetic aperture sonar images.' *Proc. Institute of Acoustics* (UK), Vol. 24 (2), 2002.

[10] D.W. Hawkins, *Synthetic aperture imaging algorithms: with application to wide bandwidth sonar,* PhD Thesis, University of Canterbury, New Zealand (1995).

[11] C.J. Oliver and S. Quegan *Understanding Synthetic Aperture Radar Images*, Artech House, Boston, USA, 1998.